THE URBAN BOUNDARY LAYER IN MONTREAL

T. R. OKE
Dept. of Geography, University of British Columbia, Vancouver, B.C., Canada
and
C. EAST
École de Santé Publique, Université de Montréal, Montréal, P.Q., Canada

(Received 17 November, 1970)

Abstract. Horizontal and vertical sampling of the atmosphere has provided new information on the form of Montreal's urban heat island. The horizontal pattern under clear skies with light winds shows a major heat island, with marked gradients at the periphery, and a multicellular inner core. Retarded urban cooling rates in the evening yield a maximum heat-island intensity around midnight. Combined horizontal and vertical temperature surveys show that under conditions of strong rural stability, the lowest layers of the urban atmosphere become progressively modified as air moves toward the centre of the city. The change in the form of the potential temperature profile is in good agreement with Summers' internal boundary-layer hypothesis. In Montreal differing heights of heat and SO_2 emission appear to produce more than one internal layer. SO_2 observations, and heat input calculations reveal two major emission sources in Montreal; one associated with an industrial complex, and the other with the downtown core.

1. Introduction

The urban heat island effect has been the most widely documented urban climatological phenomenon. However, until recently it has received only limited in-depth analysis. Recent awareness of our almost total ignorance concerning urban atmospheres has spurred renewed interest in the field. In particular the temperature structure has received increased attention because of its role in buoyancy and stability considerations when formulating atmospheric dispersion models for urban areas.

The most important new advances in our knowledge of urban temperature fields have been related to the vertical dimension. Until about five years ago our only information on the vertical extent of the urban heat island was based on balloon soundings by Duckworth and Sandberg (1954) in San Francisco, and a few fixed mast observations (e.g., DeMarrais, 1961). Since then we have learnt much from helicopter surveys in New York (Davidson, 1967; Bornstein, 1968), in Frankfurt-am-Main (Georgii *et al.*, 1968) and in Cincinnati (Clarke, 1969).

These more recent studies have shown the applicability of the mathematical model of the urban boundary layer proposed by Summers (1964) for Montreal. Summers' model simulates the passage of stable rural air across a warmer urban surface. The input of heat continually modifies the lowest part of the atmosphere, which combined with the effect of increased roughness, forms an adiabatic mixing layer over the city. The depth of this layer is considered to increase with distance from the urban/rural boundary.

Boundary-Layer Meteorology **1** (1971) 411–437.

This paper presents a study of the heat island of Montreal. In doing so there has been an attempt to link the ground-based spatial distribution, which identifies the local anomalies, with profiles of the vertical temperature structure. In addition to providing a simple three-dimensional picture, the study also includes indications of temporal variations in the heat island. The results are viewed in the context of Summers' conceptual framework.

2. Instrumentation

Measurement of vertical and horizontal temperature and sulphur dioxide (SO_2) fields over an area the size of Montreal Island, requires considerable mobility. This was achieved by the use of 6 automobiles for horizontal temperature surveys, and a helicopter for temperature and SO_2 profiles. The sensing systems and their characteristics are given in Table I.

TABLE I

Automobile and helicopter instrumentation characteristics

Carrier	Variable measured	Instrument	Response time (sec)	Relative accuracy
Automobile	Air temperature	Aspirated shielded thermistor	0.5	0.2°C
Helicopter	Air temperature	Shielded thermistor	0.5	0.2°C
Helicopter	SO_2	Electro-conductivity system	2.0	15% ambient SO_2
Helicopter	Height	Pressure transducer	0.5	4.5 m

Three automobiles were equipped with automatic temperature recording systems. Each sensor was mounted at 1.5 m in a shield constructed from polyvinyl-chloride tubing covered with reflective tape. Aspiration at 3.5 m sec^{-1} was provided by a blower-fan, and tests showed this arrangement to give results free from heating by the car, and free from frictional-warming if the speed of the car was <70 km h^{-1}. Additional spot temperatures were gained by 3 other automobile teams using Assmann aspirated-psychrometers.

The helicopter temperature sensor was the same as that in each automobile. It was housed with the SO_2 intake in a white, metal shield 60 cm ahead of the helicopter skid. In this position there were negligible effects from the rotor, or the exhaust pipe, provided that forward speeds were >30 km h^{-1}. The pressure-height transducer was

located in the helicopter cabin. All signals were continuously monitored by an electronic recorder.

3. Site and Field Operations

Figure 1 is a map of Montreal and environs including generalized land-uses. Montreal is an island-city located at the confluence of the St. Lawrence and Ottawa rivers. The city lies in the St. Lawrence Lowland region (slope $< \frac{1}{2}°$) which is interrupted by a few volcanic hills. Mount Royal is one of these hills; rising 200 m above the surrounding plain, it dominates the centre of the city.

The metropolitan region of Montreal has a population of about 2.3 million, of which about one half live in the city proper, and the remainder in the adjacent suburban municipalities. The downtown centre of Montreal is located between the eastern slopes of Mount Royal Park and the St. Lawrence water-front. The park is surrounded on its other sides by the residential areas of Outremont, Mount Royal, Hampstead and Westmount. Most of the remaining municipalities have a mixture of commercial, light-industrial and residential land-uses. Each of these communities has its own residential core. Montreal is not a heavy industrial centre, and its pattern of industrial uses is not concentrated (Figure 1). There is however a concentration of oil-refineries on the northeastern end of the island.

As the data presented here are mainly from the winter season, it is of importance to mention three winter characteristics of the Montreal area. (1) The rural areas are generally snow covered, and give rise to strong inversions in the lowest layers. (2) The rivers are frozen over during the period December-April, and therefore resemble land rather than water surfaces. (3) Due to the cold winter temperatures, space-heating is widely used. Summers (1964) estimated that the total heat released by combustion processes (industrial, domestic and automobiles) during the winter was 0.218 cal cm^{-2} min^{-1} averaged over the city. This compares favourably with the estimate of 0.285 cal cm^{-2} min^{-1} given by Bornstein (1968) for the extremely dense agglomeration of buildings on Manhattan Island. This term therefore must be considered an important heat balance term, and is a function of air temperature. For an account of the general climatology of the Montreal region the reader is referred to a comprehensive survey by Powe (1969).

During surveys the helicopter and one car left Dorval airport at sunrise and moved in sequence from stations 1–12 (see Figure 1). At each site the helicopter took observations during a 70-m-radius spiral ascent up to 900 m. Just after sunrise the remaining five cars left McGill (Figure 1) and conducted closed traverses across the city, and into adjacent rural areas. It will be noted that the stations are arranged in two transects of the island; sites 1–7, and sites 8–12. The two lines cross at site 4/11.

Unless otherwise stated, standard meteorological observations are those from Dorval airport on the southwest side of the city (see Figure 1). Additional wind information was available from urban towers located on the top of Mount Royal (317 m above msl), and at the Botanical Gardens (6 and 60 m above ground). Water temperatures were supplied by the Montreal Harbour Master.

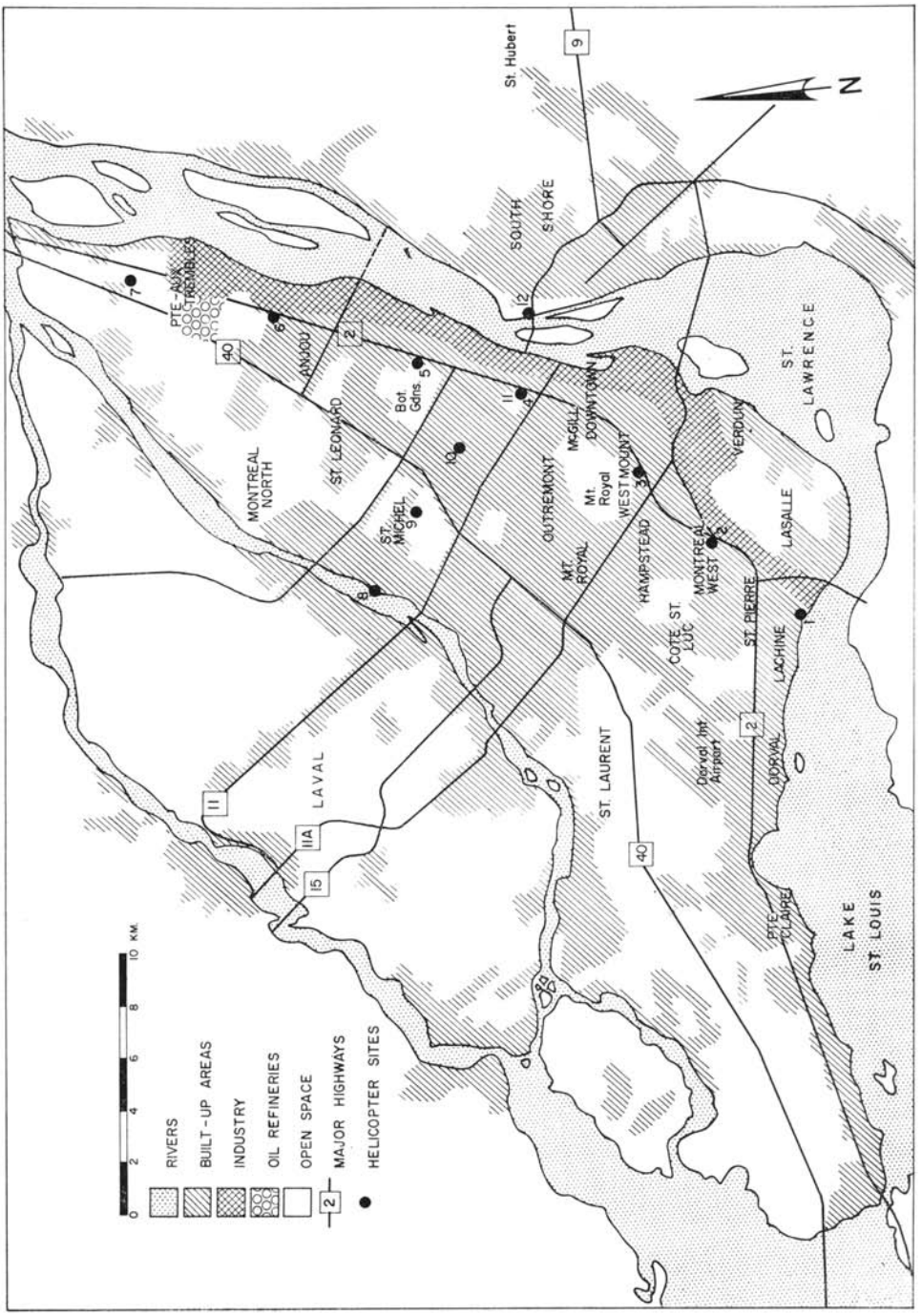

Fig. 1. Location and land-use map of Montreal.

4. Data Corrections

The scale of enquiry in urban climatology imposes problems in gathering strictly comparable data. Even using six cars it took 2 h to obtain a horizontal sample density of approximately 1 point km^{-2} over Montreal. Warming or cooling during this period makes it impossible to compare the conditions at different locations. It is necessary therefore to apply time-based corrections to the data. Equally it is imperative to apply height-based corrections to account for the effects of adiabatic cooling.

(1) Both the automobile and helicopter data were converted from environmental to potential temperature (θ), standardized to 1000 mb. Maximum ground-level corrections were applied to data from the top of Mount Royal (c. 1.5 °C); at other locations corrections were very small. Helicopter corrections were of course much larger.

(2) Time-based corrections were applied to the automobile data, based on the assumption of a linear temperature change with time. This assumption was checked with the continuous temperature records at the McGill Observatory, and was found to be reasonable. Applying this procedure throughout the survey area involves the inherent assumption that the urban warming/cooling rate is the same as in suburban and rural areas. In Section 6 this will be shown to be incorrect; corrections are thus only approximate for areas whose warming/cooling rates are different from those of the urban reference station. Using this procedure, corrections were typically of the order 0.1 °C $(10\ min)^{-1}$. Horizontal isotherm maps were then constructed based on a common time, usually 0700 Eastern Standard Time (EST).

(3) In addition to conversion to potential temperatures, the helicopter data were corrected to account for progressive heating of the lowest layers due to solar heating of the surface after sunrise. Essentially it was necessary to find the average rate at which the diurnal heating wave extended upwards. This was possible by comparing profiles from ascents Nos. 4 and 11 at the same site, observed, on the average, 78 min apart during 48 surveys. Temperature differences between the ascents at each height were calculated, and arranged in 100-m layers to provide a series of histograms (Figure 2). Also included in Figure 2 (by shaded areas) is an indication of those days when incoming solar radiation exceeded 10 cal $cm^{-2}\ h^{-1}$ during the experiments.

The frequency graphs all show normal distributions, but those for 50–100 and 125–200 m show a shift to the right of zero. This indicates predominantly warming conditions, and the similar shift in solar heating cases confirms this conclusion. For the uppermost layer (above 200 m), both distributions remain normal and are centred about zero, showing no bias towards warming or cooling, and no obvious relation to solar input. Since the mean time of ascent No. 4 was 38 min after sunrise, it was concluded from the above analysis that in the 116 min following sunrise the effects of solar heating were confined to the layer below 200 m. Since helicopter traverses started at sunrise, and the time between successive ascents was 10 min, it was decided to assume that the solar-heated layer moved 20 m upward during each ascent. Accordingly, the time-based automobile correction was assumed to decrease linearly

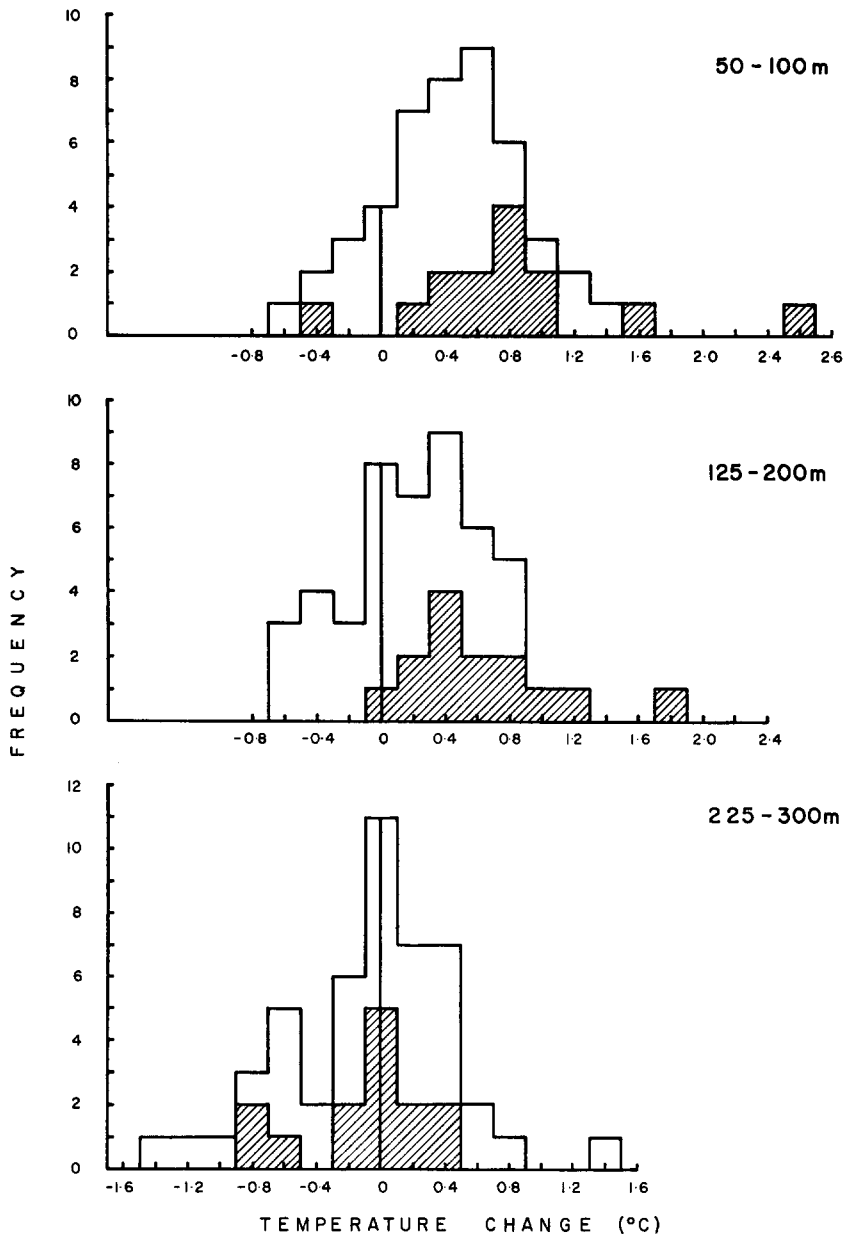

Fig. 2. Frequency distribution of temperature differences between ascents Nos. 4 and 11 organized by layers. Shaded cases indicate global radiation > 10 cal cm^{-2} h^{-1}.

from the base of each profile, becoming zero at the top of the heated layer. The method is only approximate, but appears to have worked well in practice.

Differences in the time constants for sensing temperature, SO_2 and height (Table I) could lead to inaccurate height comparisons. At an ascent rate of 3.6 m sec^{-1} the height errors for θ and SO_2 are 1.1 and 5.4 m, respectively. Allowance has been made for the relatively large time constant of the SO_2 equipment, assuming that the SO_2 readings were representative of the air at the height of the helicopter 2 sec earlier. Errors arising from the short time constant for θ lie close to the accuracy of the height measurements, and therefore no corrections were applied. No corrections were applied to the SO_2 data for time trends.

It is anticipated that the resulting temperature distributions represent an almost instantaneous picture of the lower atmosphere over Montreal, just after sunrise.

5. Horizontal Heat Island

Like so many of the world's major cities, Montreal's thermal regime is not governed simply by urban climatic factors (e.g., artificial heat production, building materials, etc.; for a review see Oke (1969)). The situation is complicated by controls such as topography and proximity to a water body. Thus the resulting heat island is unique to Montreal, and reflects its particular geographic setting. Automobile surveys provide an ideal way to investigate the areal thermal response of the city as well as these other controls, and help to elucidate the distribution of heat sources and sinks.

Two surveys have been chosen to illustrate some of the more recurrent features of the nocturnal urban heat island in Montreal during the winter months. The cases chosen are for Wednesday March 18th, 1970, and for Thursday January 23rd, 1969. The corresponding isotherm maps are given in Figures 3 and 4, respectively.

The March 18th survey was conducted in the late evening (2100 EST), following a day of clear skies and moderate winds with 18 cm of relatively fresh snow lying on the ground at Dorval. The city streets were bare with some old snow. During the survey, winds were SW at <2 m sec^{-1}, and skies were mainly clear.

From Figure 3 it is obvous that the city is producing a heat island whose intensity, ΔT_{u-r} (defined as the difference between the warmest and coolest surveyed points, excluding obvious topographic or other extraneous factors) is about 7°C (12.5°F). The urban/rural boundaries of the city produce the familiar strong temperature gradient or 'cliff' at the edge of the heat island, and the isotherms closely correspond to the built-up limits. There is evidence of cold air pushing towards the centre of the heat island with the SW wind. In general the urban/river boundaries do not show strong gradients.

The interior of the heat island is relatively complex unlike that in some previous heat-island studies (e.g., Chandler, 1965; Munn *et al.*, 1969). Inside the roughly concentric peripheral isotherms there are a series of apparently haphazardly-organized cells of both warmer and cooler air. On closer inspection, however, it is found that the cooler spots occur in open areas within the city (in this case Mount Royal Park, the

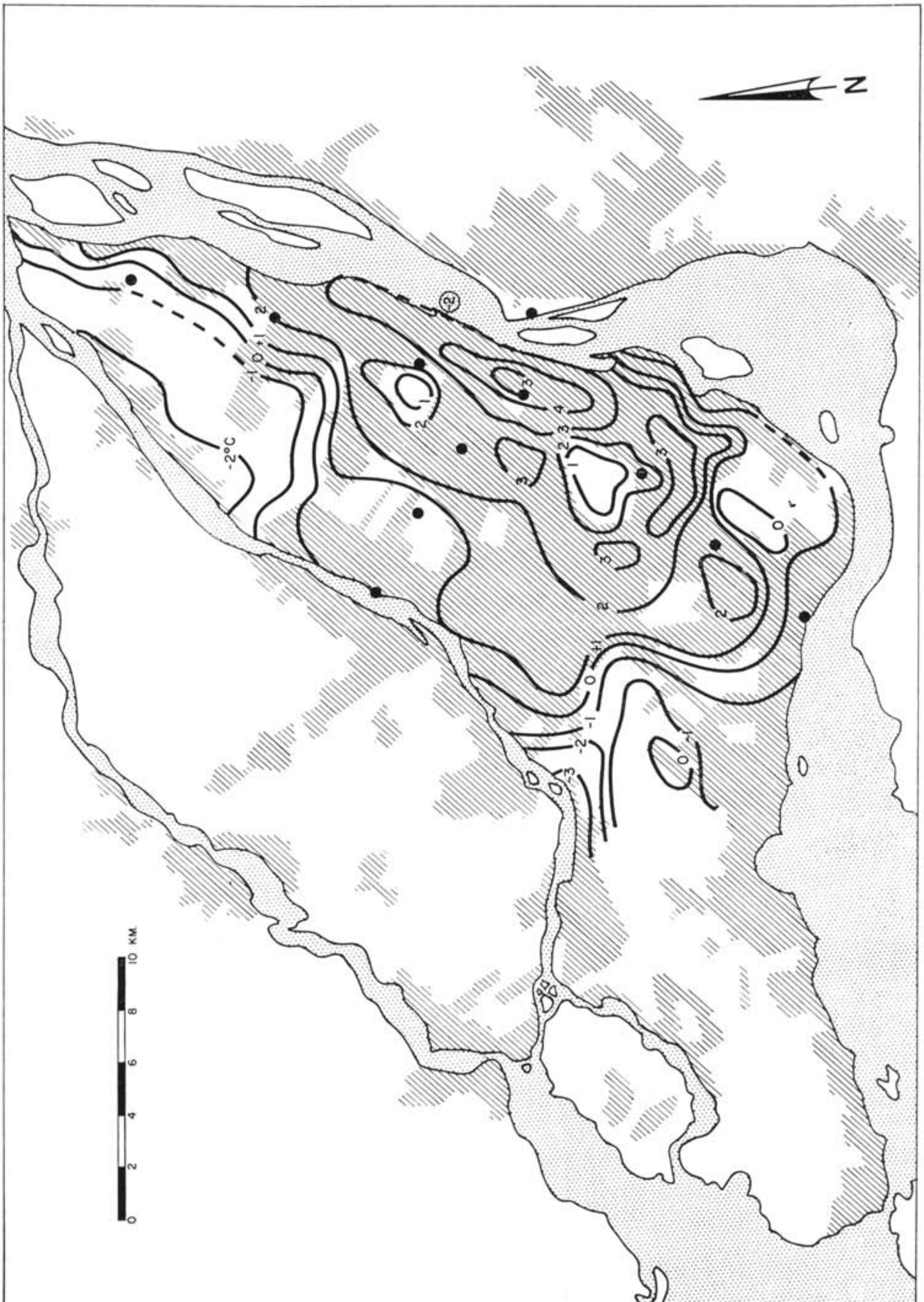

Fig. 3. Horizontal potential temperature (θ) distribution in Montreal on March 18, 1970 at 2100 EST. Isotherms are in °C. Circled reading is water temperature. Winds SW < 2 m sec^{-1}, cloud cover $\frac{1}{10}$ cirrus.

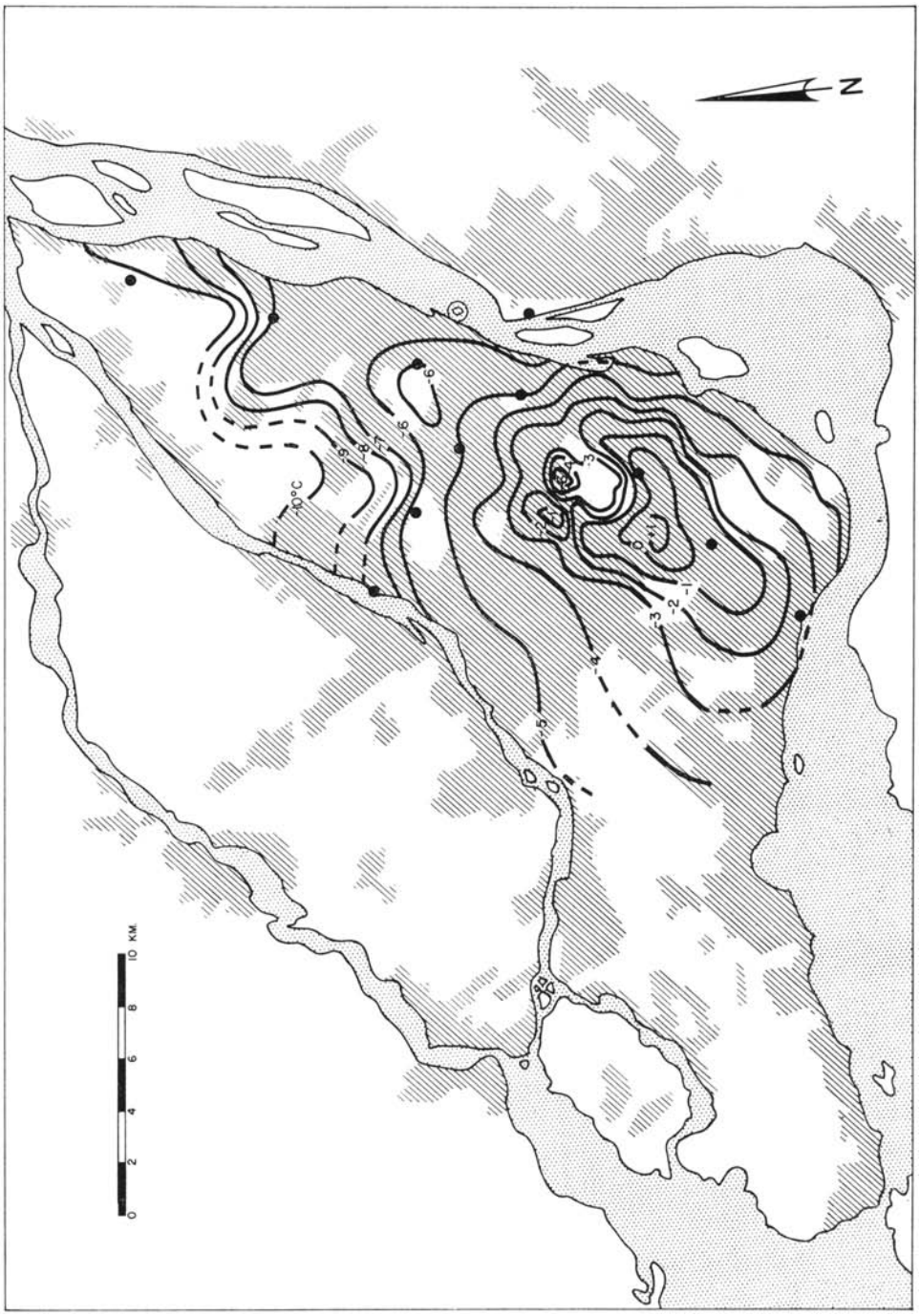

Fig.4. Horizontal temperature distribution (°C) in Montreal on January 23, 1969 at 0700 EST. Winds NE < 1.5 m sec^{-1}, skies clear.

Botanical Gardens and the open space of La Salle). It should be remembered that the Mount Royal data have been corrected for adiabatic cooling due to elevation, and thus the coolness of the area is a surface response. The warm spots correspond to the locations of community shopping areas (see Figure 1), as well as to the main downtown high-rise commercial core. Obviously this downtown core-cell has been elongated and displaced northeastward by the wind. It should also be noted that the Dorval International Airport complex is large enough to produce its own small heat island of about 2°C.

The January 23rd survey (Figure 4) refers to conditions at 0700 EST following two days of sunny, hazy weather with exceptionally light airflow (average daily wind speed 1.0–1.8 m sec^{-1}). Nocturnal winds were NE and very light at <1.5 m sec^{-1}. Skies were clear except for urban smog, and there was 41 cm of snow lying in the suburbs.

Following a period of anticyclonic stagnation with very cold rural air, the city is able to produce a heat island of about 11°C (20°F). The largest urban-rural differential achieved during these surveys was 12°C (22°F) on February 15, 1970 at 0000 EST; again air temperatures were very cold (−20°C) and winds were nearly calm. Although relatively few summer surveys have been completed, it seems certain that Montreal's heat island reaches its maximum intensity during winter. The dependence on air temperature suggests that space-heating plays a major role. The maximum value of 12°C agrees almost exactly with the maxima found in San Francisco (Duckworth and Sandberg, 1954), and Edmonton (Daniels, 1965). This value seems to constitute an upper limit for heat island intensity in temperate latitudes.

The windward urban/rural boundary again shows a well marked 'cliff' following the built-up outline. The gradient across this boundary is about 1.4°C km^{-1}, but in extreme cases gradients of 4.0°C km^{-1} have been observed in Montreal. The western and eastern boundaries of the heat island are less distinct, except in the very complex zone near the downtown core. This may depend on the fact that these boundaries are urban/river rather than urban/rural; but considering that the rivers were frozen over, it is reasonable to assume that they were acting more as land surfaces than water. It seems that the survey has not included the total area which contributes to the urban heat island. This is especially true of the eastern boundary where urbanization has spilled over onto the area known as the 'South Shore'. Cross-sectional surveys across the river and along highway 9 clearly showed the main heat island extended eastwards, to a 'cliff' near St. Hubert (Figure 1). Thus the heat island showed a conformity with the Greater Montreal limits of urbanization rather than the geographical island itself.

Figure 4 again illustrates the multi-cellular centre of the heat island. The warm cells associated with commercial centres have tended to amalgamate into a larger cell in the lee of Mount Royal. The cool cell of Mount Royal is well developed and elongated by the wind. On some calm mornings there was evidence of cold spots around the mountain due to katabatic drainage. The multi-cellular arrangement of the heat island centre is best displayed on mornings with very light winds when advection is reduced. Visual observations of chimney smoke from the helicopter confirm the

existence of these cells, and of thermal breezes across the heat-island boundaries (Yap *et al.*, 1969).

These two cases serve to illustrate conditions with near-ideal wind and cloud conditions. Two further cases in Section 7 will show some of the influences exerted by greater cloud amounts and wind speeds.

6. Warming/Cooling Rates

The heat-island maps given in Figures 3 and 4 give a static view of the spatial variation of temperature during these night periods. To gain a more dynamic picture of the way the heat island develops and dissipates, additional surveys were conducted to ascertain the relative rates of warming or cooling in urban, suburban and rural areas. Each survey consisted of a one-hour closed traverse, starting and finishing in the downtown core, and including suburban areas on the South Shore, and rural areas near St. Hubert (Figure 1). In each of these land-use types, approximately 9 stations were selected as a representative sample of conditions. By conducting surveys every hour through the night, it was possible to construct heating/cooling rate ($\Delta T/\Delta t$) graphs for each land-use, and to correlate these rates with the growth and decay of the heat island intensity (ΔT_{u-r}).

Figure 5 shows the conditions on February 14/15, 1970, a period with calm or very

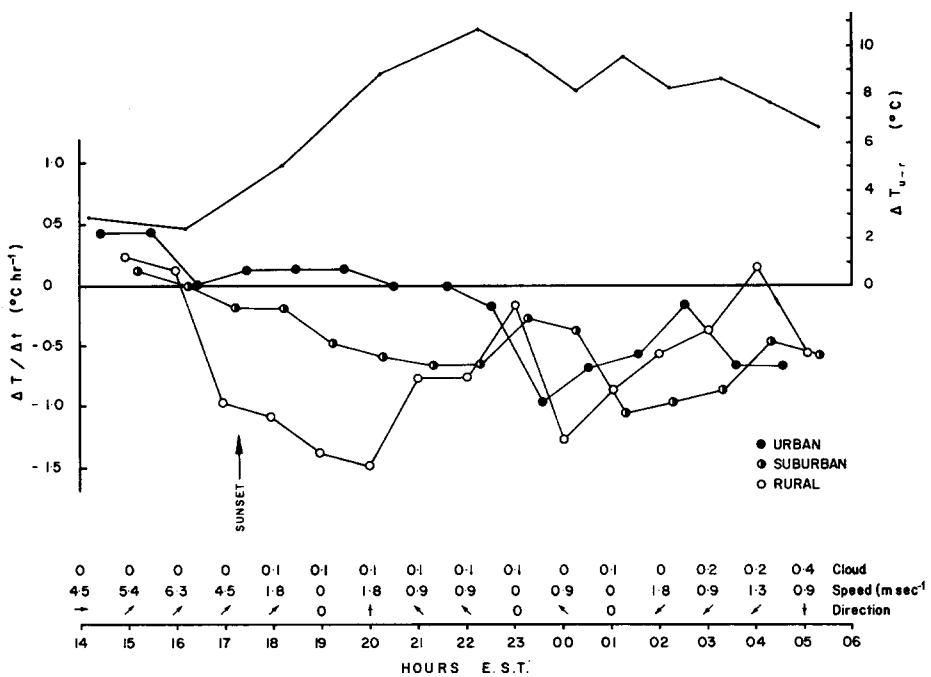

Fig. 5. Warming/cooling rates ($\Delta T/\Delta t$) for urban, suburban and rural areas in or near Montreal during February 14/15, 1970, and the related heat island intensity (ΔT_{u-r}).

weak SE winds and almost cloudless skies. The conditions therefore are considered almost optimal for heat-island development, and accordingly ΔT_{u-r} attains a value of 10.5°C (c. 19°F). As reported in Section 5 this night produced the maximum differential of 12°C. This was recorded by another survey car operating slightly leeward of the city centre. Thus the conditions depicted are extreme, but serve to illustrate the emerging picture of heat island dynamics.

From Figure 5 it can be seen that in the afternoon hours (1400–1600 EST), warming rates are prevalent in each of the land-use types, with the urban area showing a slightly higher value. About one hour before sunset, as the wind speed drops, the rural area shows a very marked change to strong cooling ($>1\,°C\ h^{-1}$). Presumably this is a result of strong surface radiational loss, and cooling of the lower atmosphere. The urban area on the other hand exhibits a thermal inertia, with temperature rates close to zero until just before midnight. It is suggested that this situation is the result of a number of urban factors all operating to offset cooling: namely, the release of heat stored in the building materials from the previous day's insolation; the stagnation of warmer air between the roughness elements; the addition of sensible heat from space heating (Dorval air temperature at 2000 EST was −17°C); and the counter radiation from the urban smog dome. The suburban situation appears to lie between the urban and rural extremes, but seems to parallel the urban trend more closely. During this period from sunset to almost midnight, ΔT_{u-r} steadily builds to its maximum value in response to the differing urban and rural cooling rates. Later in the night the cooling rates become similar, and remain fairly constant until sunrise. Presumably during this period the urban area has expended much of its stored heat, and rural surface temperatures have become low so that outgoing losses are reduced. The heat island diminishes gradually as morning approaches.

This type of analysis provides a new dimension to heat island studies, and helps to formulate a better understanding of the relative responses of urban and non-urban surfaces. There are two important consequences to this study. (1) Cooling rates in different parts of the city and surrounding countryside vary greatly. Hence the method of time correction outlined in Section 4 is only valid for the urban area, and will tend to underestimate changes in the rural areas, thus giving less intense heat islands than actually occur. (2) The 0700 EST heat island maps probably depict less than the maximum ΔT_{u-r} value, whereas that at 2100 EST (Figure 3) is probably closer to the maximum intensity for the night. Early morning surveys dominate in this paper because it was necessary to have daylight to fly the helicopter over the city.

7. Combined Horizontal and Vertical Studies

This section presents the results from four occasions when the urban heat island was studied with respect to both its horizontal and vertical extents. As such it provides the first integrated picture of an urban heat island. The chosen surveys illustrate the effects of different wind speeds and cloud amounts, and in one case the effect of a water body upwind of the city. In all cases we sought to avoid the presence of elevated

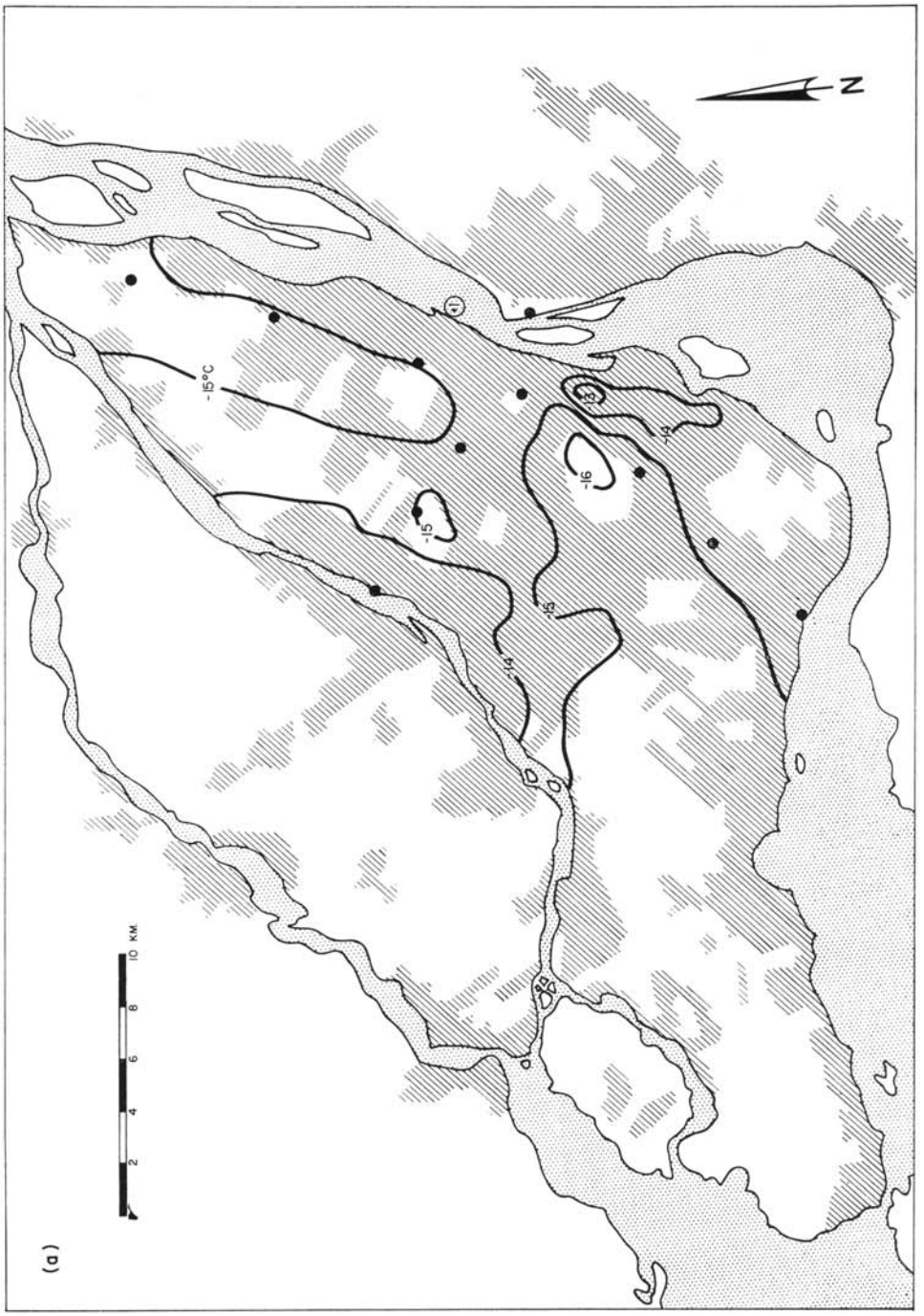

Fig. 6a.

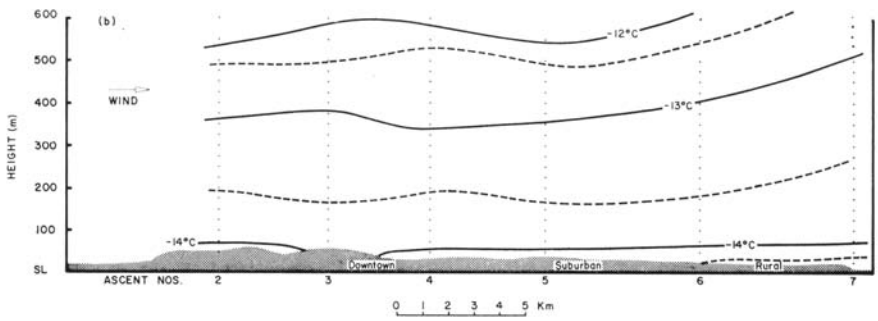

Figs. 6a–b. (a) Horizontal temperature distribution (°C), and (b) along-wind vertical temperature (θ) cross-section for February 22, 1968 at 0700 EST. Winds SW 9.4 m sec^{-1}, overcast stratus cloud.

inversions due to warm-front advection, or subsidence warming, which might confuse the urban effect.

The use of potential temperatures (θ) here, is considered important because this enables statements to be made concerning the stability or instability of an air layer, which is fundamental to discussions concerning the diffusion of aerosols. The use of uncorrected environmental temperature (T) by previous authors may be misleading since the existence of a lapse profile need not necessarily indicate good conditions for upward diffusion. The use of θ is also useful in the demarcation of the positions of any internal boundary layers which may exist in the flow.

The helicopter data extend up to 900 m. Since it appears that surface effects do not extend that high, however, the results presented here are truncated at 600 m. The link-up between the helicopter data near the surface and the automobile data is good considering problems associated with the need to land in open spaces inaccessible to the automobiles. The largest discrepancy was about 1 °C, but was usually <0.5 °C.

A. FEBRUARY 22, 1968, AT 0700 EST

This survey was characterized by strong SW winds at 9.4 m sec^{-1}, increasing to SW 14.3 m sec^{-1} at 325 m, and a low stratus overcast. The ground, especially in rural areas, was covered with 12 cm of snow, and most of the rivers were frozen over.

The isotherm map for this survey (Figure 6a) shows only a weak heat island pattern clinging to the downtown high-rise section. Cool country air is being advected across the urban area to link with the cool air over Mount Royal. The heat island is only 1–2 °C (<4 °F) and may be considered almost insignificant. This conforms to a statistical analysis which concluded that the heat island in Hamilton is obliterated if winds are >11 m sec^{-1} (Oke and Hannell, 1970).

The vertical along-wind cross-section for the same time (Figure 6b), shows the entire depth of the atmosphere up to 600 m to be weakly stable, yielding a spatially uniform temperature field, with no indication of any urban influence even in the lowest layers. It is a little surprising that with such high mechanical turbulence the air does not show neutral layers close to the surface. This is possibly attributable to

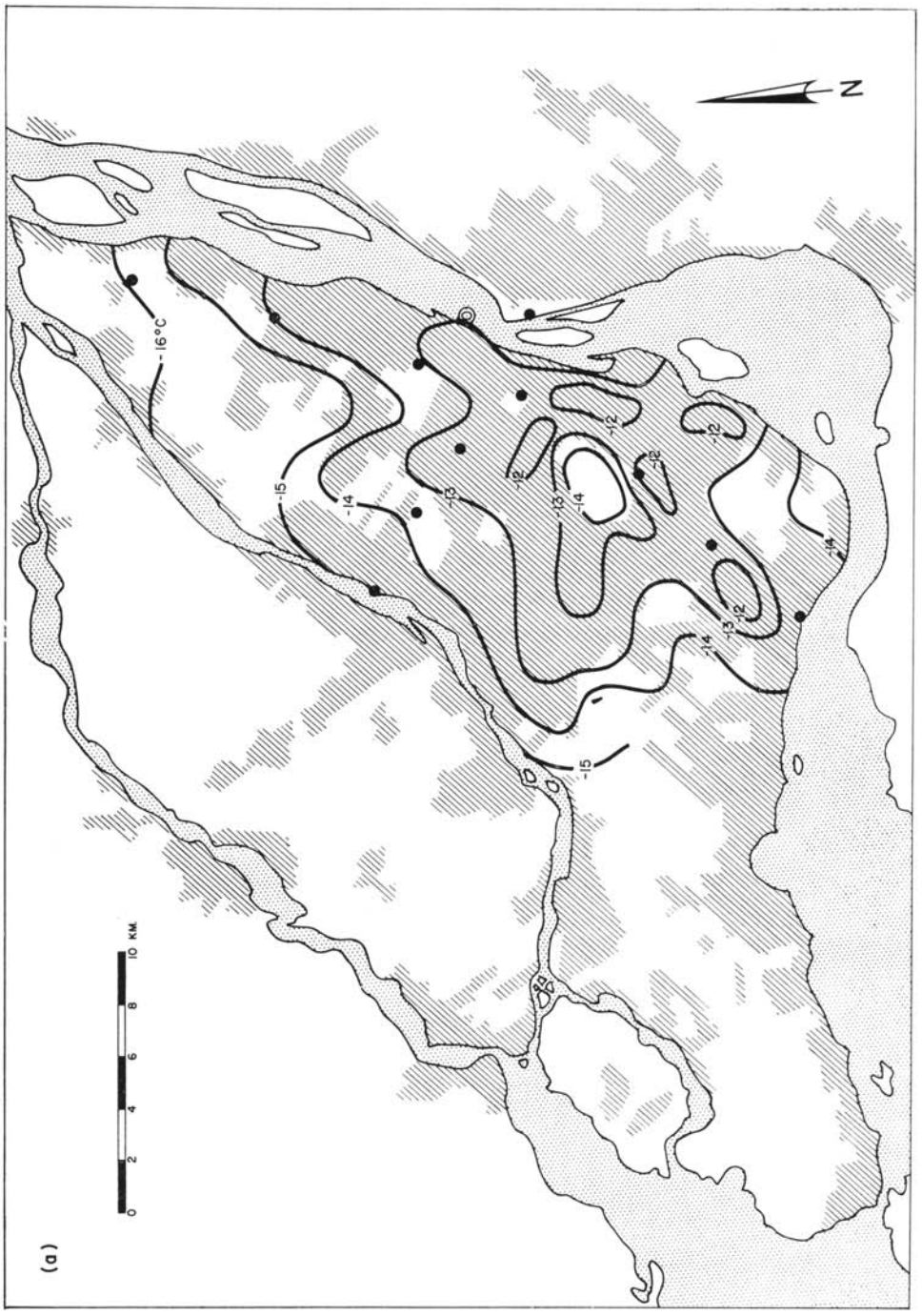

Fig. 7a.

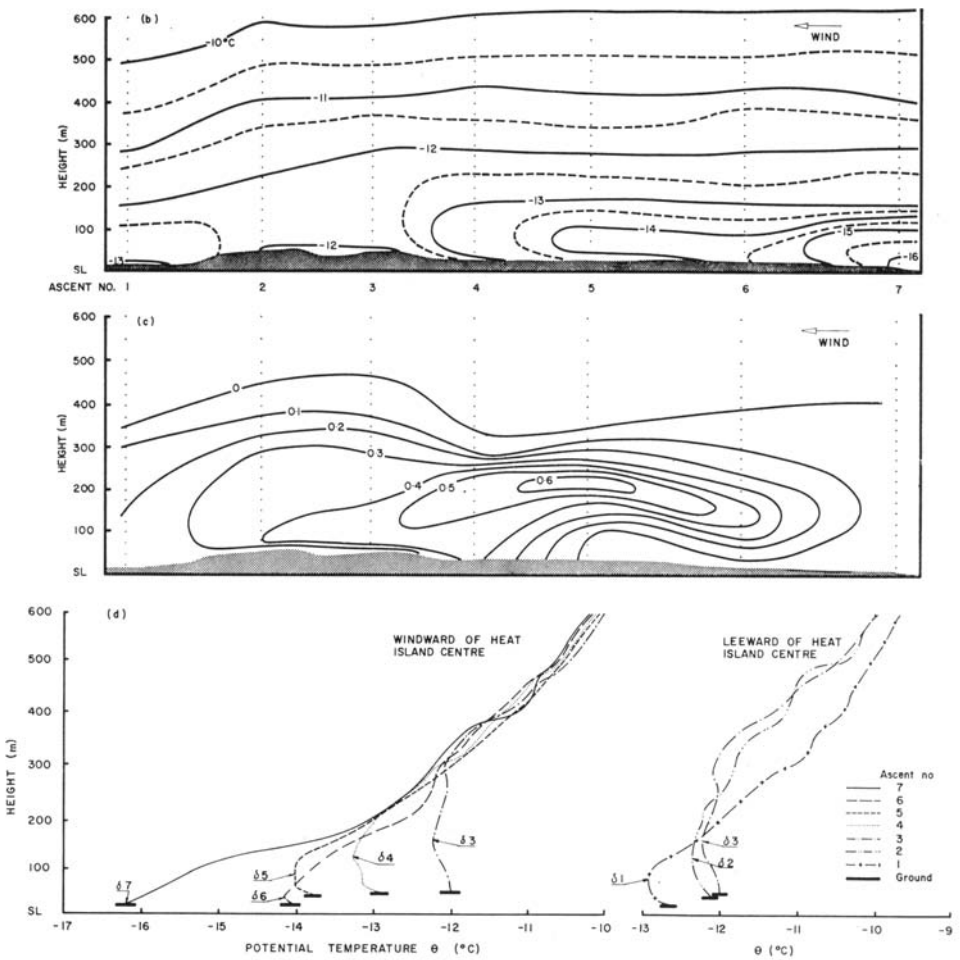

Figs. 7a–d. (a) Horizontal temperature distribution, (b) along-wind vertical temperature cross-section, (c) along-wind vertical SO_2 (ppm) cross-section, and (d) along-wind temperature profiles for March 7, 1968 at 0700 EST. Winds N 0–0.4 m sec^{-1}, skies clear.

cooling due to contact with snow surfaces for a long fetch upwind of the city. With such good ventilation, SO_2 concentrations were low, about 0.02–0.03 ppm by volume.

B. MARCH 7, 1968, AT 0700 EST

On this morning winds were N, at 0–0.4 m sec^{-1} at ground level, increasing to NE at about 4.5 m sec^{-1} at 200–300 m. The sun rose at 0630 EST and skies were clear. The surrounding countryside was thinly snow-covered and there was old soiled snow in the city.

The surface temperature map (Figure 7a) exhibits all the features of a well-developed heat island as outlined in Section 5. The urban/rural temperature difference is about

4.5°C (c. 8°F). Mount Royal produces a cool centre, surrounded by the warm core cells associated with commercial centres.

The flow from the N/NE was exactly along the main helicopter traverse route, and hence any modification of the air may be monitored as it moves from essentially rural surfaces across the urban area. Figure 7b shows that the air is progressively warmed as it traverses the urban area to its centre, and that the depth of modified air increases downwind. This is shown particularly well by the profiles given in Figure 7d. At the rural site (ascent station No. 7, see Figure 1) the atmosphere is strongly stable from the surface up to at least 600 m. As the air moves across the urban/rural boundary, the very lowest layers become unstable, and the layers above, neutral or weakly stable up to about 300 m, where the profile shape again resembles the rural profile. This modification continues to involve a greater depth of the atmosphere as the centre of the heat island (ascent station No. 3) is approached, at which point the affected layer is about 300 m deep. Below this elevated stable layer, conditions are almost neutral. Such a development almost perfectly fits Summers' urban boundary-layer model. Beyond the centre of the heat island, the present data do not clearly indicate whether the boundary layer continues to grow, or whether it diminishes as the heat input wanes.

It is interesting to note that, as reported by Bornstein (1968) and Clarke (1969), the environmental temperature picture showed a number of elevated inversions over the city. However, the use of θ eliminated these multiple inversions, by incorporating them into one deep stable layer.

The SO_2 cross-section (Figure 7c) reveals the location of the major source areas, and the influence of the urban heat island on the distribution of SO_2. The two major sources are the industrial zone (mainly oil refineries located between ascent stations 6 and 7), and the downtown area where space heating is pronounced. Maximum concentrations are found about 200 m above the surface presumably due to the combined effects of the height of release, and plume rise. Similar elevated SO_2 maxima have been observed in New York (Davidson, 1967) and Philadelphia (Davis and Newstein, 1968). Maximum ground-level concentrations (0.2–0.4 ppm) are found closer to the centre of the city where fumigation due to weak vertical mixing brings the plume to the ground. This effect is augmented by the SO_2 released from the low-level downtown chimneys whose effluents possess weaker buoyancy. The elevated stable layer restricts the SO_2 to levels below 400 m over the city-centre and lower elsewhere.

C. MARCH 12, 1968, AT 0700 EST

The conditions on this morning were very similar to those in case (B) above. Surface winds were extremely weak N/NE about 1.3 m sec^{-1} and were therefore again aligned parallel to the main helicopter traverse route. The sun rose at 0615 EST, and skies were mainly clear.

The surface heat island (Figure 8a) was well developed with a magnitude of about 4°C (c. 7°F). All the previously noted features are present, and there is a general SW shift in the isotherms. The vertical temperature pattern along wind (Figures 8b and

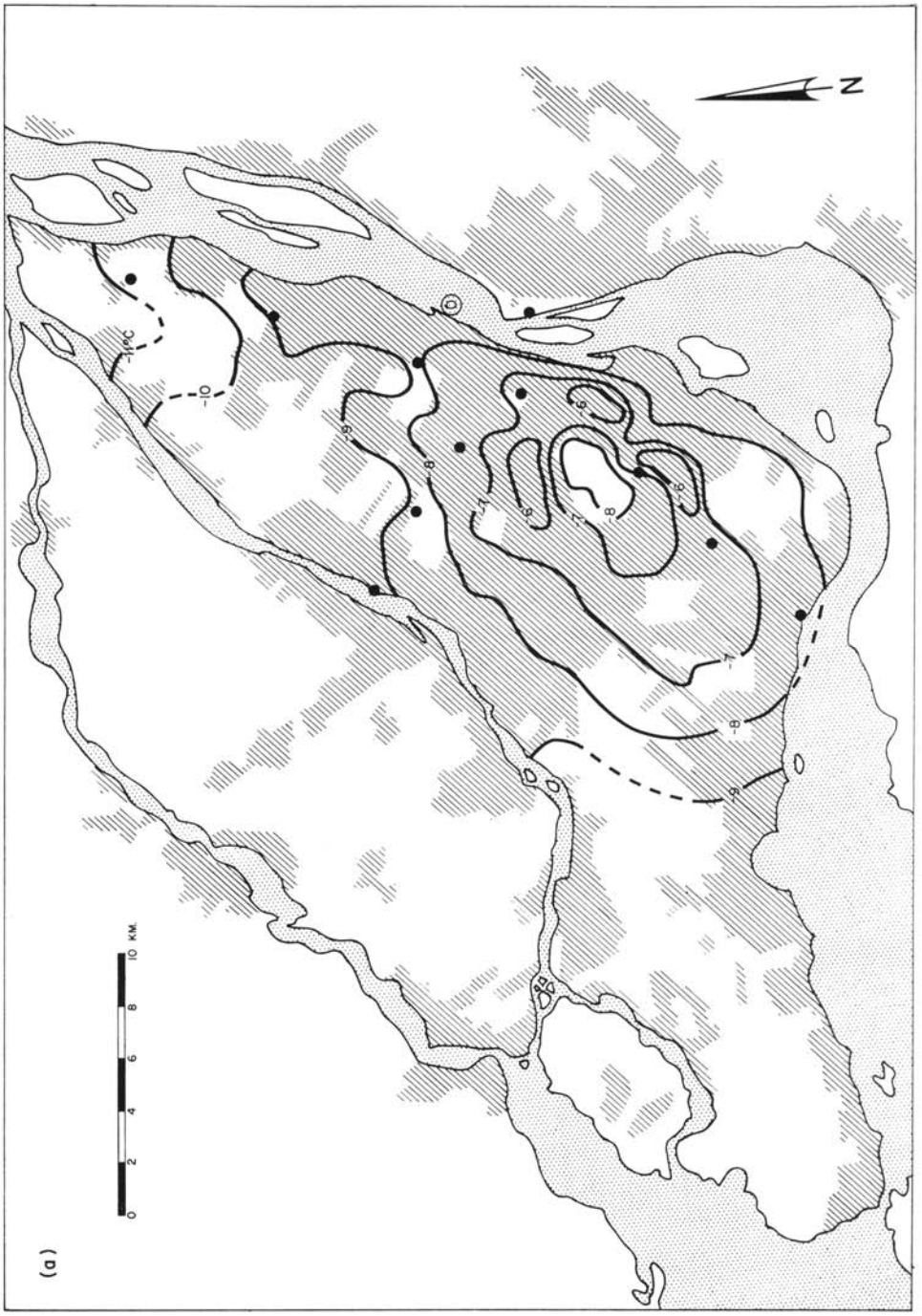

Fig. 8a.

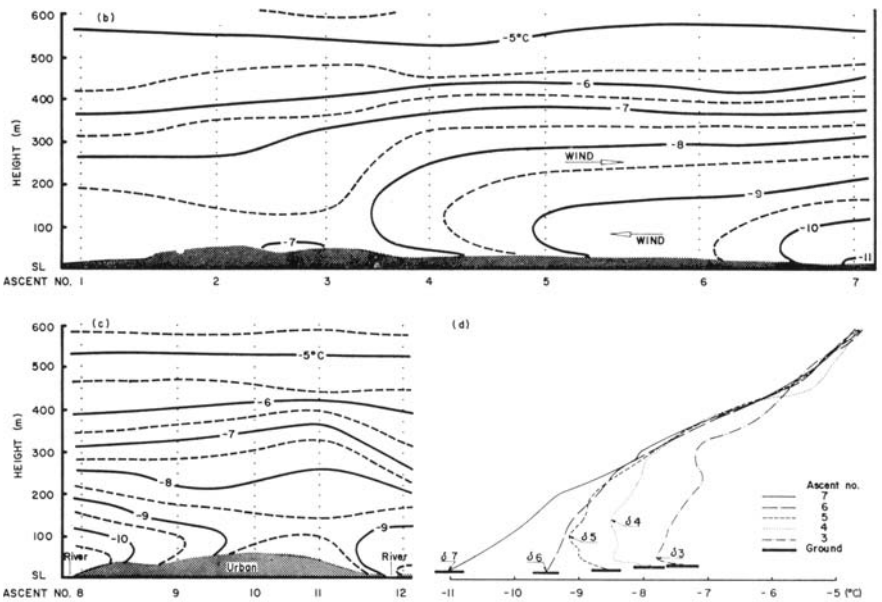

Figs. 8a–d. (a) Horizontal temperature distribution, (b) along-wind vertical temperature cross-section, (c) crosswind temperature section, and (d) along-wind temperature profiles, for March 12, 1968 at 0700 EST. Winds N/NE at 1.3 m sec^{-1}, cloud cover $\frac{1}{10}$ altocumulus.

8d) reveal a very similar situation to that outlined previously. However, on this morning there was a marked wind shear with the air at 200 and 325 m blowing from the SE, counter to the surface flow. There is evidence that the warmer air aloft is riding up over the advected country air. For this reason the production of unstable or neutral stability by the city appears to cease at about the centre of the island. Figure 8c illustrates the cross-section normal to the surface wind flow and shows that the modified layer is shallow (c. 200 m) near the centre of the island, and becomes shallower towards each river, where almost rural stability conditions are re-established.

The SO_2 pattern (not shown) is difficult to interpret because of the wind shear complication. But the two main source regions were again evident, and all the pollutants were trapped below a very stable layer based at about 300 m over the downtown core.

D. NOVEMBER 21, 1968, AT 0700 EST

This survey differs from others in this section in that it was conducted in the period before freeze-up on the St. Lawrence; hence water temperatures were above freezing. Winds were W at 3.6 m sec^{-1}, and skies were essentially clear. There was about 8 cm of snow lying in rural areas.

At this time water temperatures were about +3°C whereas rural air temperatures were about 10°C cooler. Air approaching the southwest limits of the island of Montreal had a fetch of about 18 km over Lake St. Louis and hence became modified in its

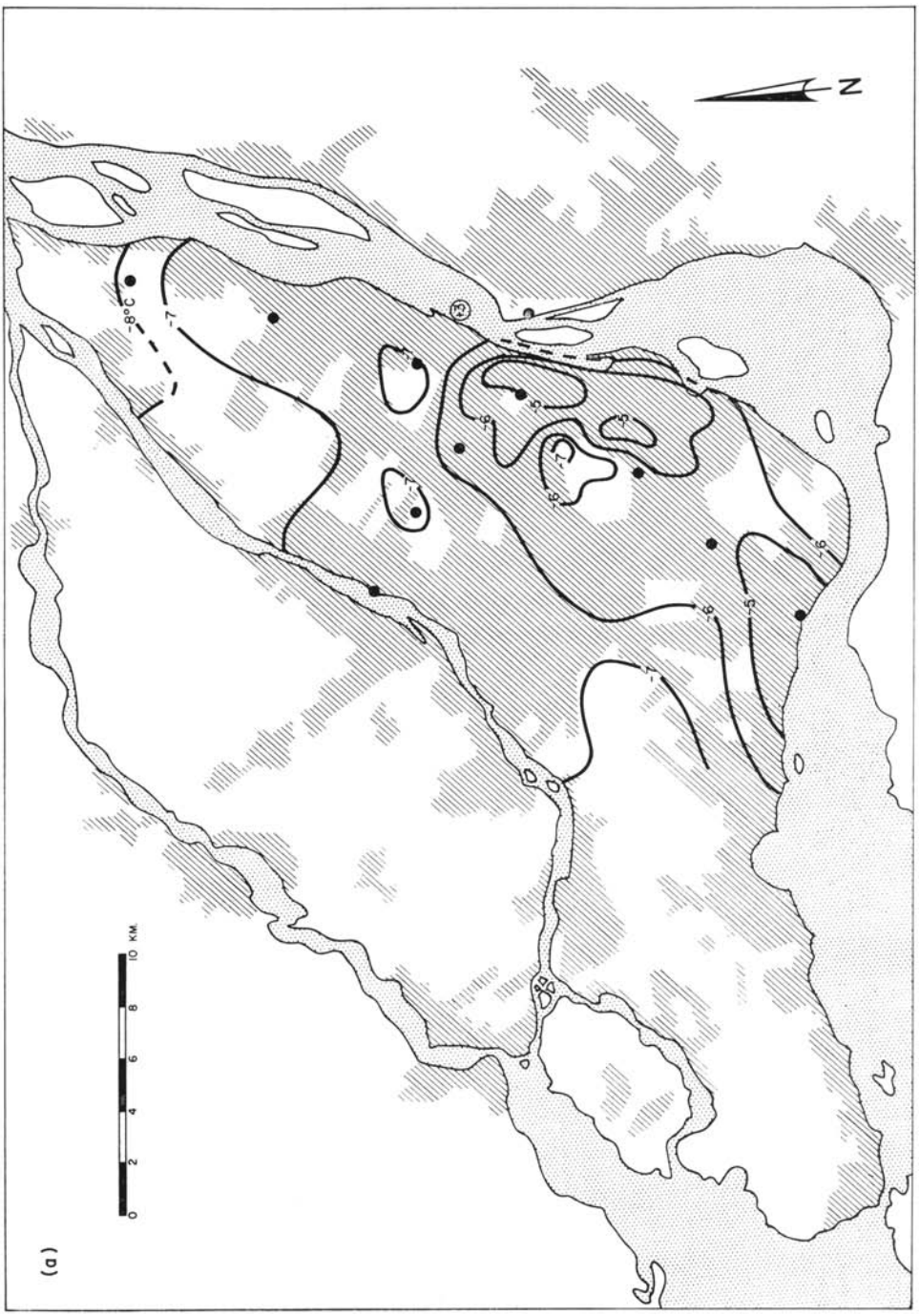

Fig. 9a.

lowest 25–50 m by this warm body of water. Figure 9a shows this incursion of relatively warm air from the west into areas of Dorval and Lachine (Figure 1). This warming produced instability in the lowest layers at ascent No. 1 (Figure 9b), but thereafter except for minor warm spots, the air continued to cool and remained stable even over the built-up sections of the city.

Because winds were W, the cross-section (Figure 9c) was not quite normal to the

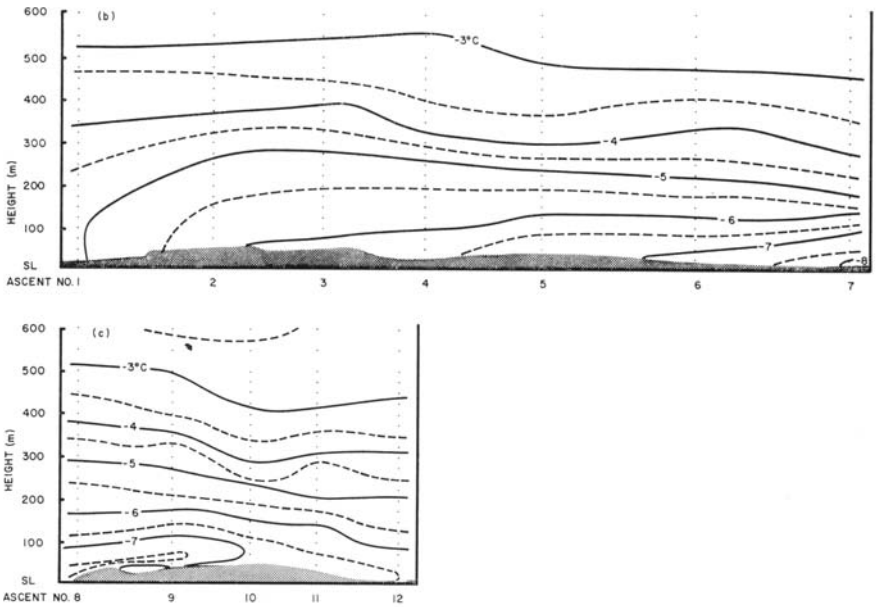

Figs. 9a–c. (a) Horizontal temperature distribution, (b) and (c) cross-island temperature sections, for November 21, 1968 at 0700 EST. Winds at 3.6 m sec^{-1}, cloud cover $\frac{1}{10}$ cirrus.

flow and thus received a component of the flow down its length. However, it will be noted that since the surfaces upwind of this line are land rather than water, there is advection of cold air across the island with some urban-induced instability in the lowest 100 m.

Also, due to the wind direction, no SO_2 concentrations were recorded from the east-end industries. However, appreciable amounts were encountered in the lowest 100 m over the downtown area.

8. Urban Boundary Layer

To gain a more general understanding of the height of the heat island in Montreal, an analysis similiar to that of Bornstein (1968) was conducted. Height vs temperature-excess graphs were constructed by taking the difference between the upwind rural ascent (No. 7) and the urban sounding most closely corresponding to the centre of the

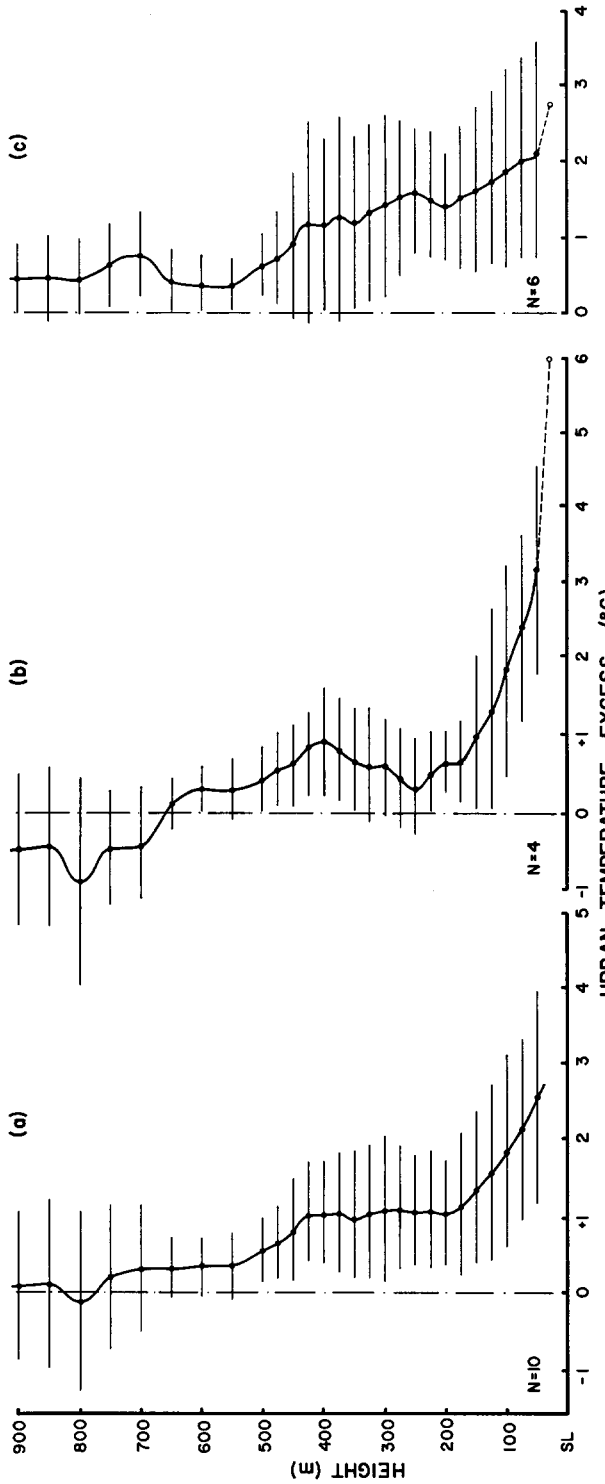

Figs. 10a–c. Height variation of urban temperature excess (°C) just after sunrise for (a) all wind speeds, (b) 0–3 m sec^{-1}, and (c) 3–6 m sec^{-1}. Bars represent $\pm$ one standard deviation.

heat island (either ascents 1, 2 or 3). Only morning surveys with winds from the N, NW or NE were used so that the rural sounding was representative. Ten such cases, selected and divided according to 3 wind-speed classes (all winds, 0–3 m sec^{-1} and 3–6 m sec^{-1}), are given in Figures 10a–c, respectively.

The generalized picture for all wind speeds shows a maximum heat island at the surface decreasing up to 200 m at which point there is a distinct break and a layer of constant excess up to 400 m, beyond which the heat-island effect may be considered negligible, approaching the accuracy of the system ($<0.3°C$). This picture is also evident on the 0–3 m sec^{-1} and 3–6 m sec^{-1} profiles with, of course, stronger heat islands under light winds, and weaker, better mixed profiles for strong winds. The light-wind case, Figure 10b, is particularly interesting because of an apparently warm bulge at about 400 m, and urban temperatures cooler than the country above 650 m. This latter phenomenon has been dubbed the 'cross-over' effect by Duckworth and Sandberg (1954), and noted also by Bornstein (1968). In the case of Montreal, the cross-over appears to occur at higher levels than previously reported, and is much less frequent than reported by Bornstein. The warming bulge at 450 m, and the 200–400 m layer of constant excess may be indicative of imperfect mixing of heat which is emitted at different levels. This possibility is explored further below.

The individual temperature profiles were examined to attempt a determination of the height of any internal boundary layers (δ) which may exist. This revealed the possibility of two internal boundary layers, and a link with the temperature excess situation noted above. (1) There is a lower boundary layer which grows relatively slowly (height/fetch approximately $\frac{1}{100}$). This layer is characterized by neutral (adiabatic), or in the lowest layers even unstable (super-adiabatic) conditions (see δ in Figures 7d and 8d). This layer strictly conforms to Summers' 'adiabatic mixing layer', and attains a height of about 200 m at the heat-island centre. (2) Above the lower layer is a second layer whose upper limit is marked by the height at which the urban profile again resembles the rural upwind profile. Hence this layer includes air modified (warmed) as it passed over the urban area, but which remains slightly stable. This boundary attains a height of 350–450 m over the heat-island centre.

This two-layer situation may again reflect the influence of two source-levels of heat input. The main heat source is the city surface which produces the lower boundary layer; and stack heat-releases produce an additional, but less effective heat input above the ground. Presumably in this case it is proper to consider the sum of the two layers as being the total urban boundary layer, but low-level emissions may find themselves trapped and mixed in the lower layer. Visual smoke observations (Figure 11 and Summers, 1964) on clear, light-wind mornings often show the tops of the tallest downtown buildings just showing through the smog, indicating a mixing height of <200 m, although individual plumes may exist above this height. These plumes may have been emitted at an effective stack-height of about 200 m at the up-wind edge of the city, and thus above the surface-controlled urban boundary layer. The chance exists, of course, that these plumes may be brought to the surface during a morning fumigation period, bringing high ground-level dosages. If the preceding

Fig. 11. View of downtown Montreal looking SE from Mount Royal on January 23, 1969 at 0830 EST (see Figure 4 for isotherm pattern, wind and cloud). Estimated top of smoke layer 185 m. Downtown COH 3.3, and SO_2 0.15 ppm.

picture is correct, then the upper boundary starting at approximately 200 m also has a height/fetch ratio of about $\frac{1}{100}$. Such a figure is in good agreement with generally accepted rule-of-thumb estimates for the growth of boundary layers.

Summers suggested a simple relation between the size of the heat island and the mixing height (h):

$$T_u = T_r + \alpha h ,$$

where T_u and T_r are the surface temperatures in the urban and rural areas respectively, and α is the potential temperature gradient in the rural area. Leahey (1969) found good agreement between predicted and observed values of h from New York data. Similarly in Montreal, if we take the cases of March 7, and March 12, 1968 we obtain predicted/observed values of 340 m/360 m and 410 m/450 m, respectively. Similarly Ludwig (1970) has demonstrated a strong relation between the rural lapse rate and the urban heat-island intensity. Through Summers' relation, simple surface heat-island measurements may perhaps be used to estimate mixing height.

Finally, an attempt was made to calculate the surface heat flux which would be necessary to produce the observed warming of the lowest layers. A simple model was

used which assumed that the change in heat content as air travelled from one station to another was completely derived from the surface along its path, and that this was reflected by the change in the potential temperature profile. This assumes that there was no net heat exchange normal to the direction of travel (i.e., the surface is infinite and homogeneous in the cross-wind direction). Finally it was assumed that there was no appreciable wind shear in the layer concerned. Cases with strong elevated inversions were chosen so that vertical losses could also be neglected. The two days best fulfilling these conditions were March 7 and March 12, 1968, and the results of heat flux computations are given in Table II.

TABLE II

Mean surface heat fluxes (cal cm^{-2} min^{-1}) computed from successive θ profiles

Date	Dorval temp. (°C)	Shortwave radiation* (cal cm^{-2} min^{-1})	Ascent Nos. 1–2	2–3	3–4	4–5	5–6	6–7
			Heat fluxes (cal cm^{-2} min^{-1})					
Mar 7/68	−14	0.24	0.11	0.01	0.21	0.04	0.05	0.18
Mar 12/68	− 8	0.17	0.01	0.01	0.23	0.11	0.06	0.15

* Jean de Brébeuf College – an urban radiation station on Mt. Royal

On both days air flow was down the main survey line and hence warming began between stations 6 and 7. On both days a major heat input occurred between 6 and 7 due to the industrial releases. Moderate inputs existed between stations 4 and 6 in a basically residential zone, followed by a major peak between 3 and 4 in the downtown area. Thereafter, values decreased rapidly, possibly as a result of lateral losses in open areas. These values seem reasonable in comparison with the artificial heat values given by Summers (Section 3), and the incoming solar radiation on a horizontal surface (Table II). Presumably some of this energy was used to evaporate water vapour from stack plumes, and some was lost in radiative cooling of pollutants. There are however, inconsistencies in the data (e.g., overall lower fluxes for March 7 even though air temperatures were lower and space heating might therefore be expected to be greater). It is felt that probably the weakest part of the analysis lies in the assumptions and quality of observations for the wind fields.

9. Conclusion

This study has shown the possibility of investigating the three-dimensional variations of a large urban heat island, and it is suggested that further work on time-variations allied to heat-balance studies will greatly enhance our ability to understand and predict city-atmosphere interactions.

The multi-cellular nature of Montreal's urban heat island centre probably occurs also in other large cities (e.g., Hamilton, Ontario (Oke and Hannell, 1970)), where

land-uses are varied. It is possible that a greater sampling density would have revealed even more hot and cold spots. These cells may have importance in producing local circulations.

Summers' boundary-layer model has been shown to have considerable merit in qualitatively describing the passage of rural air across a city. More rigorous testing may demonstrate that it is a most valuable tool for dispersion models. The two-layer model found in Montreal is probably related to the particular arrangement of sources along the wind direction chosen for testing.

Acknowledgements

This research was supported by grants from Public Health Research Grant (Project 604-7-593) Canada Department of National Health and Welfare (C. East), and from the Canadian Meteorological Service, National Research Council, and National Advisory Committee on Geographical Research (T. Oke) to whom we extend grateful acknowledgements.

We also wish to extend our thanks to the many observers who helped to gather the data and to M. Buist and L. Bourgeois, who assisted in adapting the instrumentation for the helicopter. Particular thanks are due to B. Maxwell for preparing Figure 5, and R. Fuggle and M. Gagnon for data processing.

References

Bornstein, R. D.: 1968, 'Observations of the Urban Heat Island Effect in New York City', *J. Appl. Meteorol.* **7**, 575–582.

Chandler, T. J.: 1965, *The Climate of London*, Hutchinson, 292 pp.

Clarke, J. F.: 1969, 'Nocturnal Urban Boundary Layer over Cincinnati Ohio', *Monthly Weather Rev.* **97**, 582–589.

Daniels, P. A.: 1965, 'The Urban Heat Island and Air Pollution, with Applications to Edmonton', M.Sc. Thesis, Univ. of Alberta.

Davidson, B.: 1967, 'A Summary of the New York Urban Air Pollution Dynamics Research Program', *J. Air Pollution Control Assoc.* **17**, 154–158.

Davis, F. K. and Newstein, H.: 1968, 'The Meteorology and Vertical Distribution of Pollutants in Air Pollution Episodes in Philadelphia', *Atmos. Environ.* **2**, 559–574.

DeMarrais, G. A.: 1961, 'Vertical Temperature Differences Observed over an Urban Area', *Bull. Am. Meteorol. Soc.* **8**, 548–554.

Duckworth, F. S. and Sandberg, J. S.: 1954, 'The Effect of Cities upon Horizontal and Vertical Temperature Gradients', *Bull. Am. Meteorol. Soc.* **35**, 198–207.

Georgii, H. W., Jost, D., and Shaeffer, H. J.: 1968, 'Über die räumliche und zeitliche Verteilung von Schwefeldioxid und Sulfataerosolen in der unteren Troposhäre', Scientific Report, Institute of Meteorology and Geophysics, Univ. of Frankfurt/Main, 55 pp.

Leahey, D. M.: 1969, 'An Urban Heat Island Model', Final Report, Geophys. Sci. Lab TR-69-11, School of Engineering and Science, New York Univ., 70 pp.

Ludwig, F. L.: 1970, 'Urban Temperature Fields', WMO Tech. Note No. 108, WMO No. 254 TP. 141, 80–107.

Munn, R. E., Hirt, M. S., and Findlay, B. F.: 1969, 'A Climatological Study of the Urban Temperature Anomaly in the Lakeshore Environment at Toronto', *J. Appl. Meteorol.* **8**, 411–422.

Oke, T. R.: 1969, 'Towards a More Rational Understanding of the Urban Heat Island', *Climat. Bull.* **5**, 1–20 (McGill University).

Oke, T. R. and Hannell, F. G.: 1970, 'The form of the Urban Heat Island in Hamilton, Canada', WMO Tech. Note No. 108, WMO No. 254 TP. 141, 113–126.

Powe, N. N.: 1969, 'The Climate of Montreal', Clim. Studies No. 15, Canada Department of Transport, Meteor. Branch, 51 pp.

Summers, P. W.: 1964, 'An Urban Ventilation Model Applied to Montreal', Ph.D. Thesis, McGill Univ., Montreal.

Yap, D., Gunn, K. L. S., and East, C.: 1969, 'Vertical Temperature Distribution over Montreal', *Naturaliste Can.* **96**, 561–580.